ČESKÉ VYSOKÉ UČENÍ TECHNICKÉ V PRAZE

Fakulta jaderná a fyzikálně inženýrská

Katedra dozimetrie a aplikace ionizujícího záření

Modern Fast Scintillation Materials Based on the Doped Complex Oxides

HABILITAČNÍ PRÁCE
v oboru Aplikovaná fyzika

Ing. Martin Nikl, CSc.

Praha, leden 2015

Úvodní slovo

Tato práce je komentovaným souborem publikací, které vznikaly přibližně od r. 2000 v široké národní i mezinárodní spolupráci autora při výzkumu a vývoji krystalických pevnolátkových scintilačních materiálů na bázi komplexních kyslíkatých sloučenin. Vzhledem k praktické důležitosti těchto materiálů při detekci a monitorování ionizujícího záření, urychlených nabitých částic, ale i neutronů, jmenujme zde především moderní metody lékařského zobrazování, průmyslové defektoskopie, bezpečnostní techniky ale i některé oblasti vědy samotné, především fyziku vysokých energií, je jejich výzkum ve světovém měřítku velmi rozsáhlý a intensivní.

Komplexnost výzkumu plyne ze samotné podstaty scintilačních materiálů a jejich funkce, a proto je k úspěšnému výzkumu a vývoji nutná součinnost vícero experimentálních technik, teoretických studií, ale i cílené optimalizace prakticky důležitých parametrů, která je v plném rozsahu možná především tehdy, je-li scintilační mechanismus daného materiálového systému do detailu pochopen. Z toho vyplývá potřeba vytváření rozvětvených nadnárodních spoluprací, které dokáží vytvořit potřebnou experimentální a teoretickou bázi jako předpoklad pro úspěšný návrh a optimalizaci nových nebo inovovaných materiálových systémů pro zmíněné aplikace.

Materiálová a experimentální náročnost tohoto výzkumu vyžadovala rozsáhlou finanční podporu, která byla získávána v uvedeném období z více než deseti udělených projektů z několika grantových agentur, v České republice to byla Grantová agentura AV ČR, Grantová agentura ČR a MŠMT (programy mezinárodní spolupráce), v posledních letech také Technologická agentura ČR, v zahraničí byly získány prostředky z programů NATO, INTAS a EC FP7. Jako nejvýznačnější projekty i z hlediska národní a mezinárodní spolupráce lze uvést NATO-Science for Peace, no. 973510 (2000-2004), INTAS- Position Sensitive Detectors, no. 04-78-7083 (2005-2007) a GA AV ČR – Nanotechnologie pro společnost, no. KAN300100802 (2008-2011), ve kterých byl autor hlavním řešitelem. Jako nejvýznamnější mezinárodní spolupráci, která zásadním způsobem obohatila svými technologickými výstupy tyto studie, uvádíme kooperaci se skupinou prof. A. Yoshikawy z Institute for Materials Research, Tohoku university, Sendai, Japonsko, kde jsme od r. 2002 publikovali společně přes 150 originálních vědeckých prací a presentovali obdobný počet příspěvků na mezinárodních konferencích. Na české straně byla tato spolupráce financována především z MŠMT, Program KONTAKT a AV ČR, Program podpory mezinárodní spolupráce.

Rád bych na tomto místě poděkoval jednak uvedeným grantovým agenturám za finanční prostředky, které výzkumné práce umožnily. Dále pak spolupracovníkům z domovské laboratoře v odd. Optických materiálů ve Fyzikálním ústavu AV ČR, v. v. i., kteří odvedli obrovské množství kvalitní experimentální a teoretické práce pro naprostou většinu zde komentovaných publikací, a také firmě CRYTUR spol. s r.o. (Dr. J. Houžvička, Ing. K. Blažek, Dr. K. Nejezchleb) za dlouholetou vynikající průmyslovou spolupráci. Dík patří prof. V. Múčkovi a dalším kolegům z KJCh a KDAIZ FJFI ČVUT, kteří dlouholetou spoluprací a společným vedením studentských a doktorandských prací sepsání této habilitační práce umožnili. Zvláštní poděkování zde věnuji i své manželce Nataše za pochopení a neustálou podporu v mojí vědecké práci.

V Praze, 5.1. 2015 Martin Nikl

Content

1. Introduction

Scintillator material works as a spectral and energy transformer: it converts a high energy photon from X- or gamma-ray range into a bunch of ultraviolet-visible (UV/VIS) ones, i.e. to the flash of light. Alternatively, the accelerated charged particles (electrons, protons or more heavy ions) or even neutrons can be detected through their energy deposit in the interaction with scintillator host which is again converted into the flash of light. In practice, the scintillator detector consists of two parts, namely (i) scintillating material itself and (ii) photodetector which converts the mentioned UV/VIS photons into an electrical signal I(t)[1, V1], see **Figure 1**.

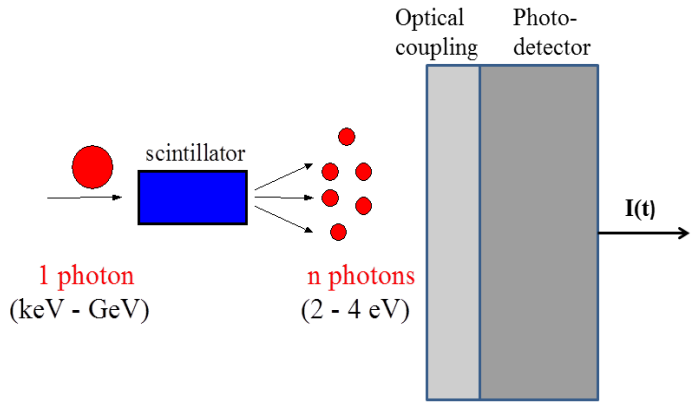

Figure 1. Principle of scintillator material and set-up of scintillation detector.

Dielectric or semiconductor wide band-gap materials are employed for such a task. Phenomenological description of the scintillation mechanism and definition of efficiency criteria have been already developed in the 1970's [2] and later further refined [3]. Scintillation mechanism can be divided into three consecutive sub-processes: *conversion, transport and luminescence*, see **Figure 2.**

Depending on the photon/particle energy, its initial multi-step interaction with the scintillator lattice occurs dominantly through (i) the photoelectric effect (below approx. 100 keV), (ii) Compton scattering effect (within 200 – 8000 keV) and (iii) pair production above the latter limit. Created hot electrons and deep holes are gradually thermalized in the conduction and valence band edges, respectively. Thermalization of carriers within the conduction and valence bands is sometimes considered as a separate stage in scintillation process due to its importance in

the study of nonproportionality issues in scintillation mechanism [4]. All the conversion process lasts typically few ps, see [4,5,6] for more detailed description. In the transport process the separated electrons and holes have to reach the emission centers, i.e. migrate through the host material: they can be repeatedly trapped or even nonradiatively recombined at trapping levels in forbidden gap arising due to lattice defects. Considerable delay in the charge carrier delivery to luminescent centers can be introduced due to such trapping processes. This stage is the least predictable as point defects, flaws, surfaces and interfaces can introduce energy levels into the forbidden gap and strongly modify/degrade scintillation performance. These phenomena are strongly dependent upon manufacturing technology [7]. During the final stage, the trapping and radiative recombination of the electron and hole at the luminescent center give rise to the desired luminescence light.

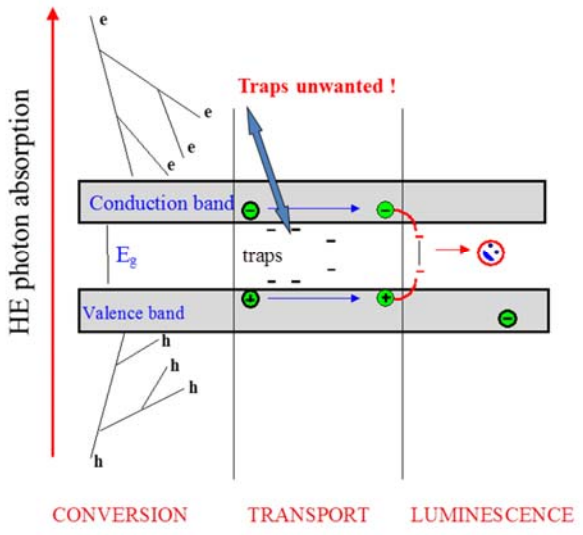

Figure 2. Sketch of scintillator mechanism in a solid state crystalline material.

The research on scintillation materials starts at the moment of X-ray discovery in November 1895 by W. C. Roentgen [8]. In the X-ray registration, simple photographic film was found rather inefficient and that is why the search for materials able to convert this new invisible radiation into visible light started immediately in order to efficiently use sensitive photographic film-based detectors. $CaWO_4$ powder was employed for this purpose just few months later in early 1896 and

together with ZnS-based powders introduced later on, these powder phosphor materials became widely used for the detection of X-rays in such combined phosphor&film detectors [9].

The history of bulk single crystal scintillators begins in the late 1940s with the introduction of NaI:Tl and CsI:Tl scintillators [10,11] which are used in a number of applications till nowadays. Since that time a number of other material systems have been reported, see [12] for an historical overview. NaI:Tl and CsI:Tl, first oxide-based $CdWO_4$ scintillator [13] and $Bi_4Ge_3O_{12}$ (BGO) [14] became widespread scintillators and are often used as "standard samples" to evaluate new materials under study. Within last two decades there has been a considerable activity in this field triggered mainly by the need of high energy physics in 1990's to find new scintillator for Large Hadron Collider calorimetric detectors which brought the optimized $PbWO_4$ scintillator [15,V2]. The advanced imaging and dosimetric applications in medicine [16] established scintillation ceramics [17] in computed tomography (CT) and Ce-doped orthosilicates in positron emission tomography (PET) [18,19]. Various high-tech industrial applications use aluminum perovskite and garnet scintillators [V2, 20]. Most recently the homeland security application call for materials of special composition for neutron detection [21,22]. Absolute majority of new single crystal scintillators, reported in this period, is based on the Ce^{3+}-doped and Pr^{3+}-doped materials, due to the short decay time (typically 10-60 ns) and high quantum efficiency of the 5d-4f radiative transitions of these centers at room temperature and in some cases even at much higher ones [23], for a broader recent survey of materials see [V3].

Despite the identical underlying physics, scientific communities working on phosphors and scintillators have been partially separated, mainly due to the different demands of related applications and different preparation technologies employed [24, 25]. In general, materials are called phosphors when applied in the photon integrating (steady-state) detection mode, while scintillators are employed in the (*X*- or γ-ray) photon counting regime. At present, the separation between phosphor (powders) and scintillator (bulk) materials is somewhat suppressed as some materials are used in both detection modes, in powder, bulk or other forms, depending on the application.

In the case of scintillators, *X* (γ)-ray photon counting consists of accumulating the generated light arriving soon after the initial conversion stage is accomplished (**Figure 2**), since the scintillator works as a high-energy photon counter. Significantly delayed light such as that due to

retrapping processes mentioned above cannot be technically exploited in the counting mode. The most important characteristics of scintillation materials are following:

(i) *Scintillation efficiency*
(ii) *Light yield (LY)*
(iii) *Linearity of light response with the incident X(γ)-ray photon energy – energy resolution and nonproportionality*
(iv) *X(γ)-ray stopping power*
(v) *Scintillation response in time*
(vi) *Spectral matching between the scintillator and photo-detector*
(vii) *Chemical and mechanical stability*
(viii) *Radiation resistance*
(ix) *Price*

The overall scintillation efficiency of *X* (*γ*)-ray-to-light conversion is determined both by intrinsic and extrinsic material characteristics. The number of UV/visible photons, N_{ph}, produced in the scintillation conversion per energy *E* of incoming *X* (*γ*)-ray photon can be expressed as [2,3]:

$$N_{ph} = \frac{E}{\beta E_g} \times SQ \qquad (1)$$

where E_g represents the forbidden gap of the material, *S* and *Q* are quantum efficiencies of the transport and luminescence stages respectively, and β is a phenomenological parameter which is typically found between 2 and 3 for most materials. The relative efficiency can then be obtained as:

$$\eta = \frac{E_{vis} N_{ph}}{E} \qquad (2)$$

where E_{vis} is the energy of generated UV/vis photons. The most efficient material among the phosphors and scintillators today is ZnS:Ag with $\eta \sim 0.2$ and even more efficient materials could still be found within those with the narrower bandgap below 3 eV.

The LY of a scintillator is always a value inferior to that given by eq. (1) since it represents only a fraction of generated visible photons, namely those arriving to the photo-detector within a certain time gate defined by the detection electronics (so called shaping time) after the high energy photon absorption. The values of shaping time are usually set between 100 ns and 10 μs.

More detailed description of other scintillator characteristics can be found in [V3].

2. Scintillators based on complex oxide compounds

The first single crystal oxide scintillator, namely $CdWO_4$, was reported around the same time as the above mentioned CsI:Tl halide one at the beginning of 1950's [13]. This material as well as all the below mentioned material systems are prepared by the Czochralski method, the principle of which is sketched in **Figure 3**. The Czochralski method [26] is one of the very few melt growth techniques of single crystals that are frequently used in industry due to favourable combination of quality, dimensions, and cost of the produced crystals. This method belongs to the oldest and most developed ones: an adequate understanding of the physical phenomena observed during solidification process has been achieved and enabled its practical expansion into the industrial large scale production. It allows controllable formation of single-crystalline cylindrical ingots of various inorganic scintillation materials The review has been recently published summarising the results of Czochralski growth of a number of scintillation materials [27].

Bulk single crystals of all the below described material systems in Section 2 are grown from the melt using the Czochralski method, see the sketch in **Figure 3**. Due to their high melting temperature above 1700°C, iridium crucible must be used. The crucible is heated by the inductive radio-frequency (RF) system. The crystal diameter is controlled using an automatic diameter control system that is operated using a signal received from the weight sensor. Typical growth atmosphere is Ar or N_2 in order to prevent oxidation of iridium crucible. Only in same cases e.g. in gallium-containing garnets growth, few percent of O_2 is admixed in order to prevent the decomposition of β-Ga_2O_3. Typical growth rate is around 0.1 - 1mm per hour.

In the melt growth of crystals using Czochralski or Bridgman methods, the dopant is distributed inhomogeneously along the crystal growth axis due to segregation phenomenon. For instance, in the case of Ce-dopant in $Gd_3Ga_3Al_2O_{12}$ (GGAG) host, the segregation coefficient $K(Ce^{3+}) = 0.36$ is considerably greater than that in $Y_3Al_5O_{12}$ (YAG) host where $K(Ce^{3+})=0.082$

[28]. These observations demonstrated that GGAG crystals accept the Ce-dopant much more easily than those of YAG that is very reasonable conclusion considering large size of the Ce^{3+} cation and greater lattice parameter of GGAG compared to that of YAG.

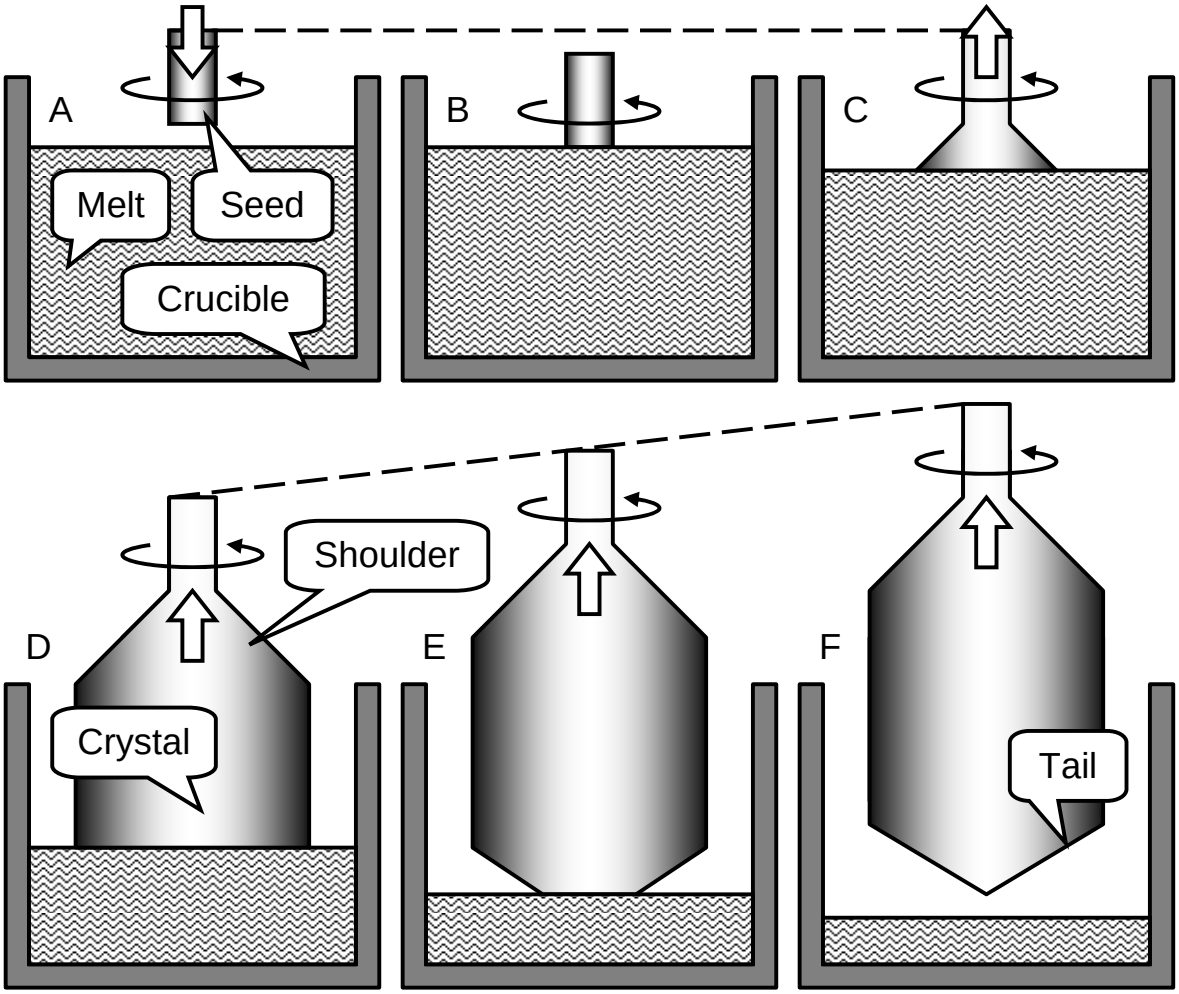

Figure 3. *Phases of typical Czochralski process including (A) approaching the seed towards the overheated melt surface, (B) immersion of the seed into the melt and their thermal equilibration, (C) pulling of the seed in upward direction with a continuous increase of the crystal diameter and shoulder formation, (D) steady state of the pulling the crystal of constant diameter, (E) ending the growth with continuous diameter decrease, and (F) separation of the crystal form the melt and its following cooling to room temperature. See also [27].*

All the below described material systems in Section 2 belong to fast scintillators where the radiative transition is based on 5d-4f emission of Ce^{3+} or Pr^{3+} ion. 5d-4f transition in these ions is completely allowed and typical photoluminescence lifetimes are within 20-60 ns and 8-20 ns, respectively. Consequently, scintillation response is dominated by similar decay time values.

Due to carrier trapping in the transfer stage of scintillator mechanism slower components are present as well.

2.1 Aluminum and multicomponent garnet scintillators

Single crystals of $Y_3Al_5O_{12}$ (YAG) were grown already in 1960's [29] and 5d-4f photoluminescence decay kinetics of the Ce^{3+} and Pr^{3+} centers in single crystal YAG host was reported soon after [30] revealing the absence of nonradiative thermal quenching up to about 550 K and 250 K, respectively. The potential of Ce^{3+}-doped YAG single crystal for fast scintillators was revealed several years later [31]. The first comprehensive description of YAG:Ce scintillator characteristics was reported by Moszynski et al [32], who included this material among the high figure-of-merit oxide scintillators. Isostructural $Lu_3Al_5O_{12}$ (LuAG) has a higher density and effective atomic number Z_{eff} (6.67 g/cm^3, Z_{eff}= 63) than YAG (4.56 g/cm^3, Z_{eff}= 32.6), which is critically important in the case of hard X- and γ-ray detection. To obtain fast scintillator the Ce and Pr-doped LuAG grown from the melt became of systematic interest in year 2000 [P1] and 2005 [P2], respectively. Contrary to YAG host, 5d-4f emission of Pr^{3+} is not thermally quenched arond room temperature in LuAG one and radioluminescence spectra indicated the absence of quenching up to at least 450 K. This characteristics together with short decay time of Pr^{3+} center (20 ns) made the LuAG:Pr R&D immediately hot topic. Recently, more precise temperatures of the onset of photoluminescence thermal quenching for Ce^{3+} [P3] and Pr^{3+} [33] centers in LuAG host were reported. The temperature at which the decay time obtained from single exponential approximation has dropped to half of the value at the plateau before the initial drop occurs is about 790 K and 680 K, respectively, which points to their possible usage at high temperature applications. Very soon in the research of these modern, highly efficient scintillators the problem of trapping electrons at shallow traps in the transfer stage was recognized [P4]. Considerable importance was given to the re-trapping and delayed recombination processes occurring in the LuAG:Ce scintillator, while the energy transfer from the trapped exciton state to the Ce^{3+} centers appeared relatively inefficient. Intense slow components in scintillation response due to the delayed radiative recombination process at emission centers were reported [P5, 34] the relative intensity of which is higher in LuAG:Ce. Based on the comparison of thermoluminescence (TSL) glow curves measured below room temperature at melt grown (T_{melt} ~ 2000 ^{0}C) and flux grown (T_{flux} ~1000 ^{0}C) crystalline LuAG:Ce, see **Figure 4**, the nature of these traps was proposed as due

to the antisite Lu_{Al} defects in the garnet structure. Such defects are due to the natural lattice disorder strongly arising with preparation temperature [35]. Their concentration can be as high as several tenths of percent and is influenced also by the host stoichiometry [36].

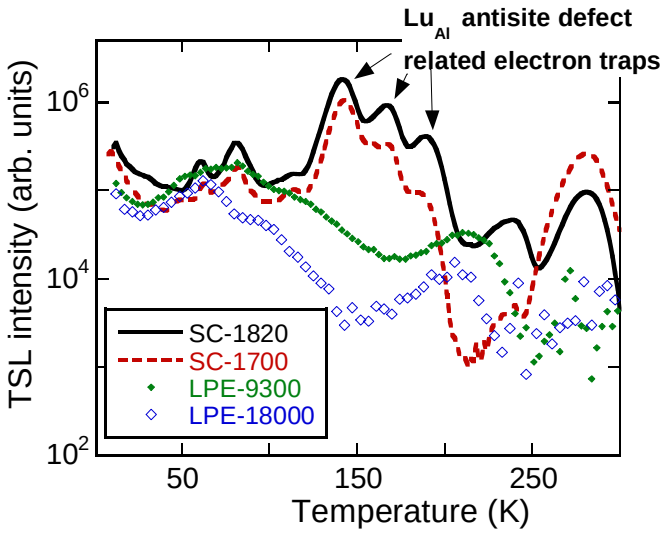

Figure 4. TSL glow curves of the LuAG:Ce single crystals SC-1820, SC-1700 and Liquid Phase Epitaxy grown films LPE-9300 and LPE-18000 samples after X-ray irradiation at 10 K. Similar X-ray irradiation doses were applied to all the samples. See also [37].

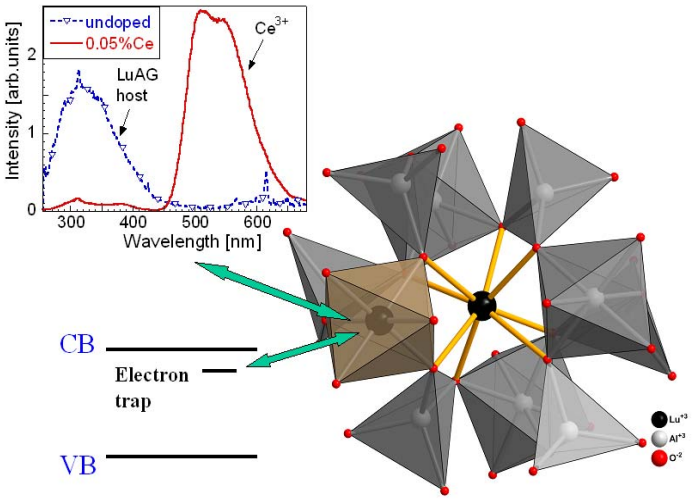

Figure 5. The Lu_{Al} (Y_{Al}) antisite defect in the LuAG (YAG) structure. Resulting electron trap in the material forbidden gap is sketched on the left. Emission band within 300-350 nm due to antisite defect and its competition with that of the Ce^{3+} center can be derived from radioluminescence spectra at RT - upper left. Emission lines around 312 nm and 615 nm in the undoped sample are due to Gd^{3+} and Eu^{3+} accidental impurities, respectively. See also [P6].

The effect of the antisite Lu_{Al} and Y_{Al} defects in LuAG:Ce and YAG:Ce scintillation mechanism, respectively, is in fact twofold [P6], see **Figure 5**, as they give rise to: (i) slower emission centers in UV region peaking at RT within 300-350 nm, which create an unwanted competitive de-excitation pathway in addition to Ce^{3+} (Pr^{3+}); (ii) shallow electron traps, which effectively delay the radiative recombination at the fast emission center and strongly degrade scintillator timing characteristics and LY value.

Furthermore, it was found that agglomeration of these traps and Ce^{3+} (Pr^{3+}) centers occurs which gives rise to tunneling-driven radiative recombination of an electron from the trap and hole localized at Ce^{3+} center. Such a process gives rise to the inverse power time dependence of the slow component in the scintillation decay of Ce^{3+} and Pr^{3+} doped LuAG at room temperature, see **Figure 6**. Deeper electron traps around the antisite defect and presumably higher concentration of these defects in LuAG with respect to YAG [P6] result in a more severe delay in energy delivery to the Ce^{3+} centers in LuAG host and can thus explain the more severe LY degradation in the Lu-based garnet structure.

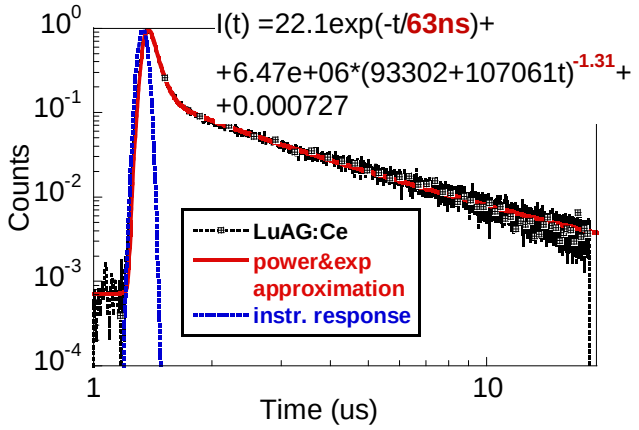

Figure 6. Spectrally unresolved scintillation decay of LuAG:Ce single crystal grown by Czochralski method. Red line is convolution of instrumental response and function I(t) displayed in the figure. The experimental decay data of [34] were used.

R&D of these garnet scintillators has been recently reviewed [P7]: as an outcome of a decade lasting intense research, new ultra-efficient single crystal family of so called multicomponent garnets $(Gd,Ln)_3(Ga,Al)_5O_{12}$, Ln = Y, Lu, doped with cerium has been discovered [P8, P9], **Figure 7**. The balanced admixture of Gd and Ga cations into aluminum garnet efficiently decreased mentioned trapping effects and prevented ionization-induced quenching of the Ce^{3+}

excited state around room temperature, see the sketch of energy levels in **Figure 8**. As a result the light yield of these materials was increased more than two times with respect to the highest performance LuAG:Ce [38]. Being currently the most efficient bulk single crystal oxide scintillators, in the latest optimized material compositions their LY is approaching 60 000 photons/MeV [39] which is a theoretical limit of these garnet scintillators [40].

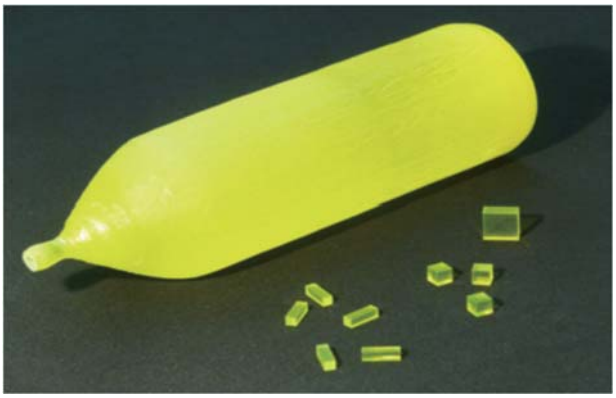

Figure 7. Photo of $Gd_3Ga_3Al_2O_{12}$:Ce single crystal, diameter 5 cm, length 15 cm. Small optical elements cut from the crystal are shown in the front (courtesy of A. Yoshikawa).

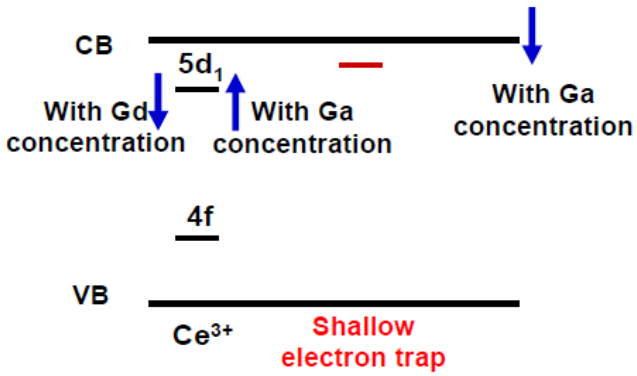

Figure 8. Sketch of energy level positioning&trends in dependence on the content of Gd and Ga concentration in $(Ln,Gd)_3(Ga,Al)_5O_{12}$:Ce, Ln = Y,Lu. See also [P8].

The decreased edge of the conduction band in these compounds due to mainly gallium admixture [P10, 41], however, considerably lowered the onset of thermal quenching in these materials which limits their usage to room temperature applications. This problem has been studied in detail and ionization of the Ce^{3+} excited state was determined as its main cause [42-44].

Interestingly, another strategy preserving high temperature stability of cerium emission centers has been recently formulated to approach the problem of electron trapping in transfer stage of scintillation mechanism in garnet scintillators with an evident positive impact on LY,

speed of scintillation response and afterglow as well. The above described modification of chemical composition of garnet scintillators results in the immersion of shallow electron traps in the bottom edge of the conduction band which diminishes charge trapping. An alternative strategy consists in creation of an additional fast radiative recombination pathway which would efficiently compete in electron trapping from the conduction band with the mentioned shallow electron traps in YAG and LuAG hosts. Such a pathway is realized by the stabilization of tetravalent Ce^{4+} center in garnet lattice by the divalent rare earth ion codoping [P3, 45-47] and/or by air annealing [48]. Positive role of Ce^{4+} in scintillation mechanism in orthosilicates have been recently reported in literature (see Section 2.3 below) and the same mechanism is apparently also functioning in garnets, **Figure 9**.

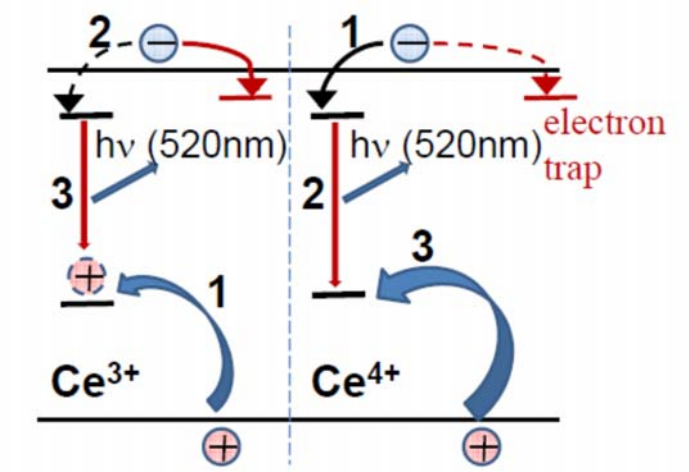

Figure 9. Sketch of the scintillation mechanism at the stable Ce^{3+} (left) and Ce^{4+} (right) emission centers in aluminum garnet host, see also [P3].

In step 1, in the first picoseconds of scintillation mechanism, the Ce^{4+} center can efficiently compete with any electron traps for an immediate capture of electrons from the conduction band. The stable Ce^{3+} center is much less effective in such competition as first it needs to capture the hole from the valence band in the step no. 1.

In step 2 the Ce^{4+}, transformed into an excited Ce^{3+} center, emits scintillation photon and contributes to the fastest part of scintillation response. In the same step the Ce^{3+} center, converted into temporary Ce^{4+}, captures an electron from the conduction band and becomes excited.

In step 3 the return into initial state (beginning of the cycle) is accomplished by the hole capture from the valence band (Ce^{4+} in the right part) and by emission of scintillation photon (Ce^{3+} in the left part).

It is worth mentioning that the last step in the Ce^{4+} scintillation mechanism (right part), the hole capture from the valence band, must always be nonradiative, i.e. not contributing to an afterglow.

Very recently, similar studies have been done for the above mentioned $Gd_3Al_2Ga_3O_{12}$:Ce (GAGG:Ce) multicomponent garnet [47, P11] Given its hight light yield, the Me^{2+} (Me = Ca, Mg) codoping does not further increase its value, but the scintillation response is apparently becoming faster, **Figure 10**, which might be of importance for applications in PET medical imaging with the time-of-flight option [19]. It is interesting to note that Ca^{2+} codoping decreases the light yield much more than Mg^{2+} codoping the reason of which has not been yet understood. Selected optical and scintillation characteristics of aluminum and multicomponent garnet scintillators are provided in Table 1.

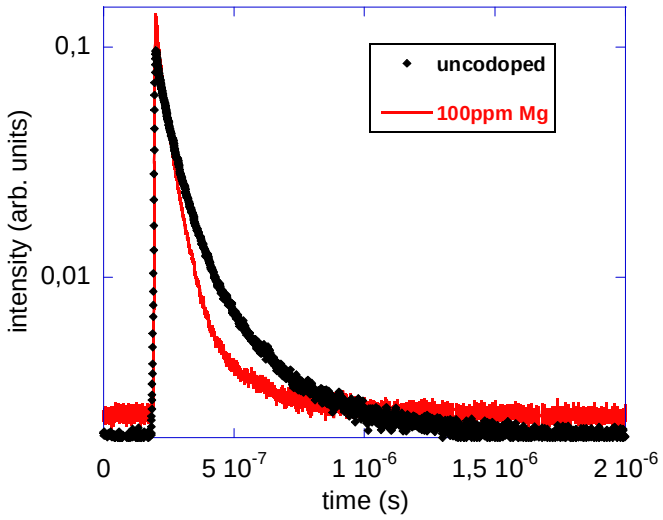

Figure 10. Scintillation decay curves of the Mg co-doped Ce:GAGG crystals [P11]. Excitation by ^{137}Cs radioisotope (662 keV). Curves are vertically shifted for clarity.

2.2 Aluminum perovskite scintillators

Fast 5d-4f uminescence of Ce^{3+} and Pr^{3+} in $YAlO_3$ (YAP) was reported by Weber [49] and Gumanskaya et al.[50], respectively. Reported lifetimes of about 18 ns and 8 ns, respectively, are among the shortest within the Ce and Pr-doped oxide-based scintillators which makes these materials attractive. Favourable properties of YAP:Ce for scintillation applications were described later by Takeda et al. [51] and Autrata et al. [52]. In the mid 1990's, similarly to what was mentioned in Section 2.1 for garnets, several laboratories paid attention to replace yttrium by

lutetium in YAP crystal to increase the density and Z_{eff} from 5.35 g/cm^3 and 32, respectively, up to 8.34 g/cm^3 and 64.9 for LuAP. Due to severe instability of LuAP perovskite phase in the process of crystal growth from the melt, see recent studies [53, 54] for further details, resulting in very high price of the crystals grown, the mixed (Lu,Y)AlO_3:Ce scintillators were finally chosen for industrial scale production [55]. These LuYAP:Ce crystals were used in ClearPET prototype [56], but did not find further commercial market due to the price and relatively lower light yield compared to YAP:Ce. The reasons for light yield decrease in Lu-rich aluminum perovskite seem to be similar as described in Section 2.1 for the garnets [P6], mainly due to the structural and chemical composition similarities. However, despite several attempts e.g. by codoping [57-59], no successful strategy has been found up to now to substantially improve it and also no successful band gap engineering of YAP by compositional variation (similarly as done in garnets [P8, P9]) has been realized [60,61] so far. Systematic luminescence characterization of Ce^{3+} center in VUV-UV spectral region in YAP and LuYAP hosts was published [P12]. Reassignement of Ce^{3+} 5d energy levels throughout the perovskite family $RAlO_3$ (R = Gd,Y,Lu), where Ce^{3+} resides in a distorted 12-coordinated cubooctahedron, has been made as well [P13]: Unlike previous intuitive suggestions in literature, calculated energy scheme manifests that two of the three low-energy levels originate predominantly from the former *Eg* doublet of an ideal cuboctahedron while the third level splits off the former *T2g* triplet. Two upper levels are predominantly formed by split levels of former *T2g*. It is worth noting that due to cuboctahedron distortion some of the resulting energy levels manifest a considerable mixing of contributions from former *Eg* and *T2g* levels. R&D results in the aluminum perovskite family were also few times reviewed [V1, V2, 62].

Given the speed of scintillation response dominated by the 8 ns decay time [63] additional effort was devoted to Pr-doped YAP to understand its 2-3 times lower light yield reported earlier [64]. The scintillation performance of a numerous set of Pr-doped YAP single crystals prepared by three different technologies including that of Czochralski, **Figure 11**, was evaluated by radioluminescence, photoelectron yield and scintillation decay measurements [P14]. The intrinsic scintillation efficiency (integral of radioluminescence spectrum) of the best Czochralski grown YAP:Pr reached about 150% of that of YAP:Ce standard sample. However, its photoelectron yield is only about 80% of that of YAP:Ce standard suggesting the presence of enhanced delayed radiative recombination processes in YAP:Pr. The discrepancy between scintillation efficiency

and photoelectron yield was systematically observed in all the Pr-doped samples. TSL measurements in the 10–350K temperature range manifest that in YAP:Pr the dominant glow curve peak occurs at a noticeably higher temperature (192 K) with respect to that found in YAP:Ce (115 K) [P14]. The calculated RT lifetime of the 192 K peak-related trap in YAP:Pr is about one order of magnitude longer (1 ms) than that related to the 115 K peak in YAP:Ce. It can be one of the reasons of the decrease of photoelectron yield in YAP:Pr due to an enhanced delay in the transport stage of scintillation mechanism. However, since the existence of the mentioned delayed radiative recombination processes in YAP:Pr is due to a defect instead of being an intrinsic property of this material, the possibilities to further optimize the scintillation performance of YAP:Pr remain open.

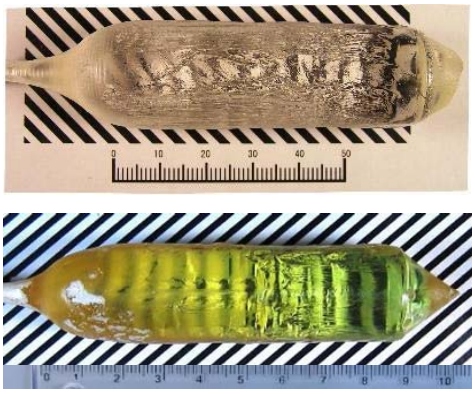

Figure 11. Photo of Czochralski grown single crystals of YAP:Pr0.5% (upper) and $Lu_{0.1}Y_{0.9}$AP:Pr1% (lower). (courtesy of A. Yoshikawa)

It is also worth mentioning the temperature stability of Pr^{3+} center in YAP, with the onset of thermal quenching above 600 K, see **Figure 12**. Applying the same criterion for the temperature of thermal quenching as in the case of Pr-doped LuAG in Section 2.1 we obtain the temperature of 690 K which is even slightly higher than that in LuAG host (680 K) indicating comparable or slightly higher thermal stability of Pr and Ce-doped YAP compared to LuAG host. Consequently, following [33] the Ce and Pr-doped Lu-admixed aluminum perovskites should show even higher thermal stability compared to simple YAP host.

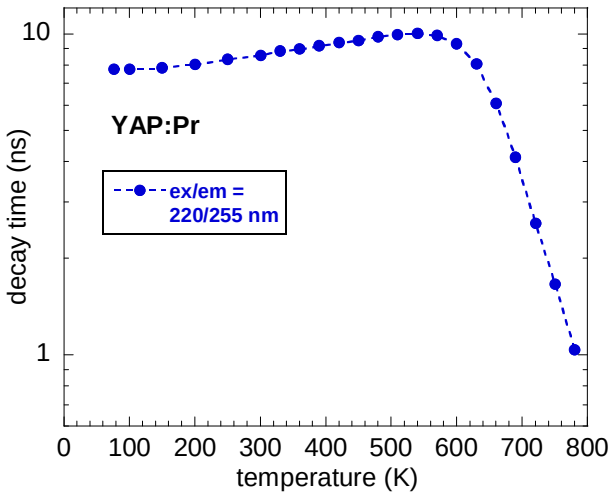

Figure 12. Temperature dependence of the photoluminescence decay time of Pr^{3+} 5d-4f emission in YAP host obtained from a single exponential approximation of the decay.

Finally, an extended correlated electron paramagnetic resonance (EPR) and TSL study of undoped and several rare earth doped YAP single crystals gave the deep insight into charge carrier trapping in this material family and its influence on transfer stage of scintillation mechanism [P15, P16]. In addition to two already known O^- hole centers [65], four other O^- centers were identified arising by holes capture from the valence band by oxygen anions. The centers differ by their thermal stability characterized by thermal activation energy E_a starting from 0.024 eV (most probably self-trapped hole) up to more than 0.5 eV which makes the most stable one surviving even at room temperatures for a few days. The holes are most probably stabilized by an impurity ion at the Y site or a cation vacancy. Electronic-type trapping sites are assigned to the yttrium antisite ions which become paramagnetic Y_{Al}^{2+} centers after trapping an electron. They are found in four structurally different configurations with a thermal stability around or higher than 300 K that enables the radiative recombination of thermally liberated holes with such localized electrons. In two of the centers, the trapped electron is additionally stabilized by an oxygen vacancy. Yttrium antisite positions in YAP lattice were directly identified by ^{89}Y nuclear magnetic-resonance measurements [P16].

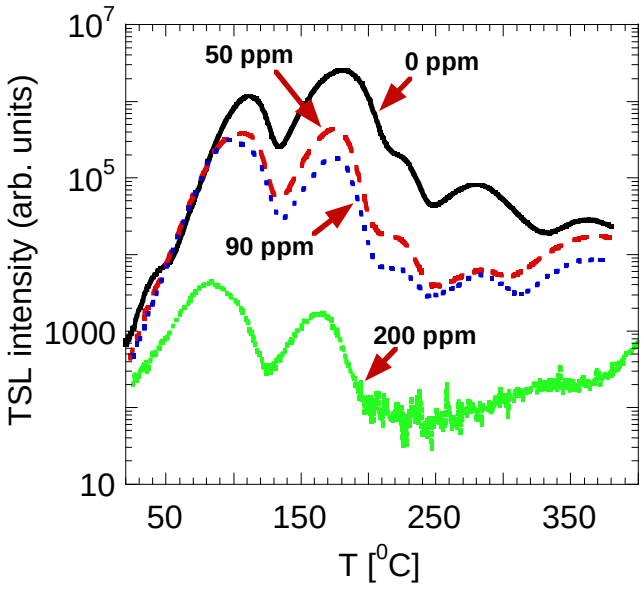

Figure 13. TSL glow curves of Zr-codoped YAP:Ce after X-ray irradiation at room temperature. Zr concentration in at. ppm is given in the figure.

Agglomeration of a deep electron trap based on oxygen vacancy with Ce^{3+} emission center and resulting thermally assisted tunneling processes in radiative electron-hole recombination were also evidenced in YAP and LuYAP hosts by TSL study above room temperature [66]. Diminished oxygen vacancy and related deep electron trap concentration evidenced by TSL glow curves above room temperature, see **Figure 13**, was achieved by the Zr^{4+} codoping of YAP:Ce single crystals. The mechanism of its functioning is very probably analogous to that in La^{3+} doped $PbWO_4$: the excess positive charge in the cationic sublattice introduced by the (co)dopant diminishes the anion vacancy creation in the process of crystal growth, see also [V2, 67]. Though scintillation response could be accelerated up to some extent, no improvement of light yield was observed [P17].

Selected optical and scintillation characteristics of aluminum perovskite scintillators are provided in Table 1.

2.3 Ortho and pyrosilicate scintilators

Scintillation characteristics of the Ce^{3+}-doped rare earth oxy-orthosilicate, namely Gd_2SiO_5:Ce (GSO:Ce) were reported for the first time in 1983 [68] and those of Lu_2SiO_5:Ce (LSO:Ce) were introduced in 1992 [69]. Later on they became well known and commercially successful single

crystal scintillators due to favourable combination of high density, effective atomic number and fast scintillation response dominated by decay time of several tens of nanoseconds further completed by mechanical and chemical stability. Their fundamental optical and luminescence characteristics including Y_2SiO_5:Ce (YSO:Ce) were provided by Suzuki et al [70] revealing two Ce^{3+} emission centres, so called Ce1 and Ce2, embedded in two sites of the RE^{3+} cation in the orthosilicate structure, **Figure 14**, and showing emission bands at about 400-440 nm and 500 nm, respectively. LSO:Ce crystals, however, identically with LuAG or LuAP-based ones described above, exhibit an intrinsic background signal of a few hundred Hz/cm^3 due to the presence of radioactive isotope ^{176}Lu, while GSO:Ce or YSO:Ce does not show such a disadvantage. Consequently, GSO:Ce can be used in low-signal-count-rate applications such as hard X(gamma)-ray astronomy [71]. Thanks to higher temperature stability of the Ce1 center in GSO host, it is widely used in oil well industry and geophysical explorations up to 150 ^{0}C at least, even if its light yield is less than half of that of LSO:Ce due to thermal quenching of Ce2 site above 200 K [70, P18]. On the other hand, optimized LSO:Ce and especially yttrium-admixed LYSO:Ce (introduced in year 2000 [72]) show the light yield exceeding 30 000 phot/MeV and are used in the latest generation of scintillation detectors in PET imaging [19]. Large crystals up to 8 cm in diameter and 20 cm in length have been grown, **Figure 15** [73]. Due to an early excited state ionization of both Ce1,2 centers [74, P19], however, they cannot be used in the applications above room temperature. The Y-admixture, among others, increases the temperature of the onset of this ionization process for both Ce1,2 centers which positively influences afterglow and day light sensitivity of this Ce-doped orthosilicate scintillators [P20]. Pr^{3+}-doped LSO was also studied [75]: At 80 K the excitation into the lowest $5d_1$ level around 250 nm results in the bright and fast structured luminescence band within 260 and 350 nm with 25 ns lifetime. At room temperature there is a considerable decay time shortening to 6-7 ns accompanied by only mild emission intensity drop. The effect is explained by an ionization of the relaxed excited $5d_1$ state of Pr^{3+} at room temperature involving an escape of an electron into the conduction band followed by the delayed radiative recombination with the Pr^{4+} center. Heavy Pr^{3+} center ionization at room temperature thus excludes the application of LSO:Pr as a fast and efficient scintillator. Structural, optical, luminescence and scintillation characteristics of these orthosilicate materials have been recently reviewed [V3].

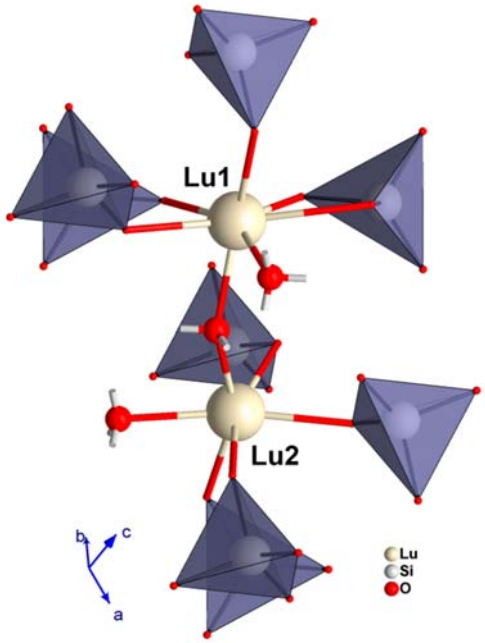

Figure 14. The structure of LSO displaying two Lu sites and surrounding SiO_4 tetrahedra. Three oxygen ions with cut bonds form OLu_4 tetrahedra and do not participate in Si-O bonds

Figure 15. Crystal of LYSO:Ce, diameter 72 mm, length 155 mm grown in Shanghai Institute of Ceramics CAS. China. (courtesy of D. Ding)

The solid solution between Ce-doped LSO and GSO hosts, so called LGSO:Ce, was discovered as an efficient, dense scintillator with the high light yield, fast decay, and weak afterglow [76-78] In the systematic compositional study the phenomenon of light yield improvement for intermediate mixed crystal compositions was demonstrated [79] which frequently appears in scintillator solid solution materials [80]. LGSO may possess monoclinic P21/c or C2/c structures depending on Lu/Gd ratio in the host. Comparative advantage of

LGSO:Ce in comparison with LSO:Ce or GSO:Ce in terms of the overall figure-of-merit is most evident around room temperature [P18].

Recent studies of the LSO:Ce and YSO:Ce scintillators have shown that Ca^{2+} codoping plays a positive role in their performance [81-83], but the detailed explanation of the underlying physical mechanism was not proposed. In 2013, a detailed study of the effect of Me^{2+} codoping in LYSO:Ce was published in which the optical and photoelectron (XANES) spectroscopy techniques were combined to evidence the presence and explain the role of stable Ce^{4+} center in the scintillation mechanism [84]. In fact, the charge transfer (CT) absorption characteristics of Ce^{4+} center in LSO in UV spectral region were revealed already a time ago in LSO:Ce [85] and found and discussed also as for the Ce^{4+} participation in scintillation mechanism in Ce-doped silica glass [86]. The absorption fingerprint of stable Ce^{4+} center provides very sensitive tool to reveal its presence in oxide hosts. In fact, very similar values of the onset of this CT absorption process in the orthosilicates and above mentioned aluminum garnet structures, see **Figure 16**, provide a strong support for such an interpretation. The Me^{2+} codoping and annealing in air [87] stabilize the Ce^{4+} center which positively influences several scintillation characteristics, namely light yield, speed of scintillation response and afterglow. This center forms new fast radiative recombination pathway based on the immediate electron capture from the conduction band, radiative de-excitation of the excited Ce^{3+} center and a hole capture to return to the Ce^{4+} stable initial state as has been sketched and described for garnet scintillators in Section 2.1 and **Figure 9**. Such a mechanism works in parallel with the standard one based on the stable Ce^{3+}center. Consequently, these two centers do not compete with each other when their relative ratio is optimized which seems to be a critical moment using this tool in material optimization [P3].

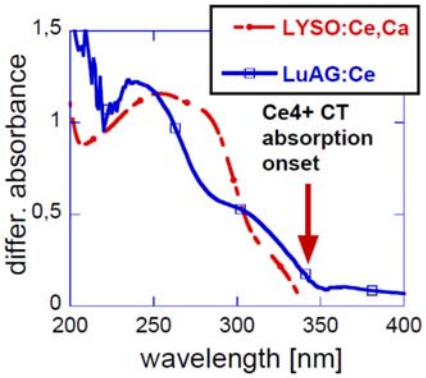

Figure 16. The Ce^{4+}-related induced absorption in Ce-doped LYSO and LuAG single crystals, see also [P3].

More than a decade ago lutetium pyrosilicate $Lu_2Si_2O_7$ (LPS) was also found as potentially interesting scintillator host [88]. Comparative EPR study of the Ce^{3+}-doped LSO and LPS showed that the Ce ion in LPS structure substitutes for Lu in its single crystallographic site while in the structure of LSO it is found in both Lu crystallographic sites [89]. The light yield of LPS:Ce single crystals, which were grown from the melt, can reach the value comparable to that of LSO:Ce, the dominant scintillation decay time is around 37 ns with no observable afterglow [88,90]. Furthermore, similarly to LSO:Ce post-growth annealing in air at elevated temperatures was found efficient in increasing the scintillation efficiency [91]. The lack of afterglow in LPS:Ce in contrast to its observation in LSO:Ce was correlated with the significantly higher temperature maxima of TSL glow peaks above room temperature [92].

More recently, $Gd_2Si_2O_7$:Ce (GPS:Ce) pyrosilicate has been introduced showing much higher light output and faster scintillation response compared to GSO:Ce [93]. GPS:Ce shows an incongruent growth from the melt [94], but heavy Ce-doping (at least 10 mol %) in GPS host does enable its congruent growth [95]. However, at such a high Ce-concentration, the light output is significantly reduced because of the self-absorption and concentration quenching. An optimal cerium concentration in oxide hosts is usually within 0.1 - 1 at. %. The congruent crystal growth of GPS:Ce is achieved by expansion of average ionic radius in the Gd site resulting from Ce-doping. At the same coordination number the La^{3+} ion has very similar ionic radius as Ce^{3+} so that the substitution of La for Ce can also be applied to stabilize the pyrosilicate phase avoiding unwanted concentration quenching of Ce^{3+} emission. The optical and scintillation properties of $(Ce_{0.01}, Gd_{0.90}, La_{0.09})_2Si_2O_7$ were reported for the first time by Suzuki et al [96] where these single crystals were grown by the floating zone method under argon atmosphere. Using Si-avalanche photodiode detector, excellent values of light output of 41.000 ± 1000 photons/MeV and FWHM energy resolution at 662 keV of 4.4 ± 0.1% were achieved [97]. The impact of La and Sc admixture in GPS:Ce prepared by the top seeded solution growth with SiO_2 self-flux was also studied regarding their structure, optical and scintillation properties [98].

Figure 17. Photo of Ce-doped GPSLa30% single crystal grown by Czochralski technique. (courtesy of A. Yoshikawa)

In the very recent study [P21] the absorption spectra, photoluminescence spectra as well as decays, and selected scintillation characteristics were studied for Ce-doped LPS, GPSLa30% and GPSLa48% single crystals grown by the Czochralski technique, **Figure 17**. The $4f - 5d_x$, x = 1 – 5, Ce^{3+} absorption bands in GPSLa30% were determined at 338, 320, 294, 242 and 219nm, respectively. The $5d$ - $4f$ emission of Ce^{3+} is peaking at 377 nm and 372 nm in LPS and GPSLa hosts, respectively. The very onset of nanosecond decay times shortening appears around 380 K (LPS:Ce) and 440 K (both GPSLa30%:Ce and GPSLa48%:Ce) and is due to thermally-induced excited state ionization. The Ce^{3+} ionization onset favourably occurring well above RT provides an opportunity to exploit LPS:Ce and particularly GPSLa:Ce in high temperature applications. Evaluated scintillation efficiency (integral of radioluminescence spectrum) reach about 250 %, 1210 % and 1530 % of that of BGO single crystal standard for LPS:Ce, GPSLa48%:Ce and GPSLa30%:Ce, respectively. In the latter compound the efficiency is almost doubled with respect to that of commercial high performance LYSO:Ce,Ca [99]. Afterglow of La admixed gadolinium pyrosilicates is fairly low and tends to get less intense with increasing La concentration becoming comparable to that of BGO. Taking further into account about two orders of magnitude lower intrinsic radioactivity (due to due to ^{138}La isotope, 0.09% natural abundance, $T_{1/2}$~10^{11}y) compared to Lu-based scintillators, the La-admixed GPS:Ce single crystals show a combination of characteristics highly favourable for medical imaging, oil industry and geophysical applications.

Selected optical and scintillation characteristics of silicate scintillators are provided in Table 1.

Table 1: Optical and scintillation characteristics of selected oxide based scintillators. Dopant concentration shows a typical value in the crystal. Scintillation decay time of the dominant component is provided. Shaping times of 1-4 microseconds were used in LY measurements. Intervals of values reflect those reported in literature and/or measured in the author laboratory at high quality single crystals available nowadays.

Crystal	**Density (g/cm^3)**	**Band gap (eV)**	**Ce^{3+}(Pr^{3+}) $5d^1$-4f em. (nm)**	**Ce^{3+}(Pr^{3+}) 4f-$5d^1$ abs./exc (nm)**	**Ce (Pr) conc. (mol%)**	**Scintillation decay time (ns)**	**LY (10^3 Ph/MeV)**	**Energy res. (%) @662keV**
YAG :Ce	4.56	7.5	550	458	0.2	90-100	28-30	6-7
LuAG :Ce	6.67	7.8	525	448	0.15	55-65	24-26	6-7
GGAG:Ce	6.2	6.5-7.0	540	440-450	0.3	90-170	50-58	4.2-5.2
LuAG:Pr	6.67	7.8	308	284	0.1	20-22	18-20	4.6-5
LuYAG:Pr	6.2-6.5	7.7	310	286	0.1	20-22	27-33	4.4-6
YAP:Ce	5.35	8.2	365	303	0.2	19-25	22-25	4.5-5.5
YAP:Pr	5.35	8.2	247	215	0.1	8-10	6-12	11-13
LYSO:Ce,Ca	7.2	7.2	400	357	0.1	30-35	30-32	8-9
(Gd,La)PS:Ce	5.4-5.7	6.6-6.8	365-370	338	0.3	45-50	32-36	5-6

The defects, their energy level positioning and role in scintillation mechanism of silicate scintillators have been studied comparatively less compared to garnets and perovskites described in Sections 2.1 and 2.2, respectively. Shallow trapping states are much less influencing the scintillation response which follows from absolute comparison of TSL glow curves among Ce-doped LYSO, YAP and LuAG single crystal samples [P6], see **Figure 18**, where that of LYSO:Ce shows 1-2 orders lower intensity compared to others. In fact, no noticeable slower components were reported in microsecond scale in scintillation decay of LSO:Ce or LYSO:Ce.

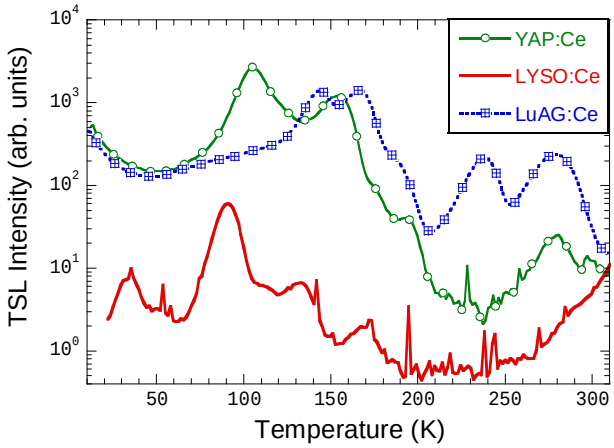

Figure 18. TSL glow curves of YAP:Ce, LuAG:Ce and LYSO:Ce after X-irradiation at 10 K. Curves can be compared quantitatively. See also [P6].

Instead, the afterglow in LSO:Ce was an issue from the very beginning of its study: Fundamental studies, aimed at the comprehension of the microscopic physical mechanism governing afterglow were thus carried out in order to find possible technological solutions. The activation energy of the process was found to be approximately 1 eV [100]; it is in accordance with the calculated trap depth of a TSL peak at 375 K so that at room temperature afterglow appears to be due to carrier detrapping from the trap responsible for this peak followed by radiative recombination at Ce^{3+} luminescent centers. Actually the 375 K peak is the first of a series of as many as 6 peaks observed in the glow curve above RT, whose spectral emission coincides with Ce^{3+} 5d-4f transition [100]. Annealing experiments in reducing or oxidizing atmosphere led to the suggestion that traps could be related to oxygen vacancies [101]. The nature of traps and mechanism of afterglow phenomena in LSO and LYSO was further addressed by detailed wavelength resolved TSL measurements above room temperature [P22]. We interpreted the presence of four glow peaks with the same trap depth, see **Figure 19** (upper part), as due to the a single electron trap located at different distances with respect to recombination centres (Ce^{3+} and Tb^{3+} rare earth dopants); the radiative recombination between electrons and holes occurs through a thermally stimulated tunnelling mechanism, see **Figure 19 (**lower part**)**. We identified oxygen vacancies as the predominant electron trap in LSO and LYSO. The ascription of traps to oxygen vacancies is based on the very good correlation of O-Lu distances (corresponding to distances between oxygen vacancies and substitutional rare earth ions) in the monoclinic *C2/c* structure of

LSO and LYSO to the frequency factors of the traps which contain the transmission coefficients of the potential barriers between trap and centres.

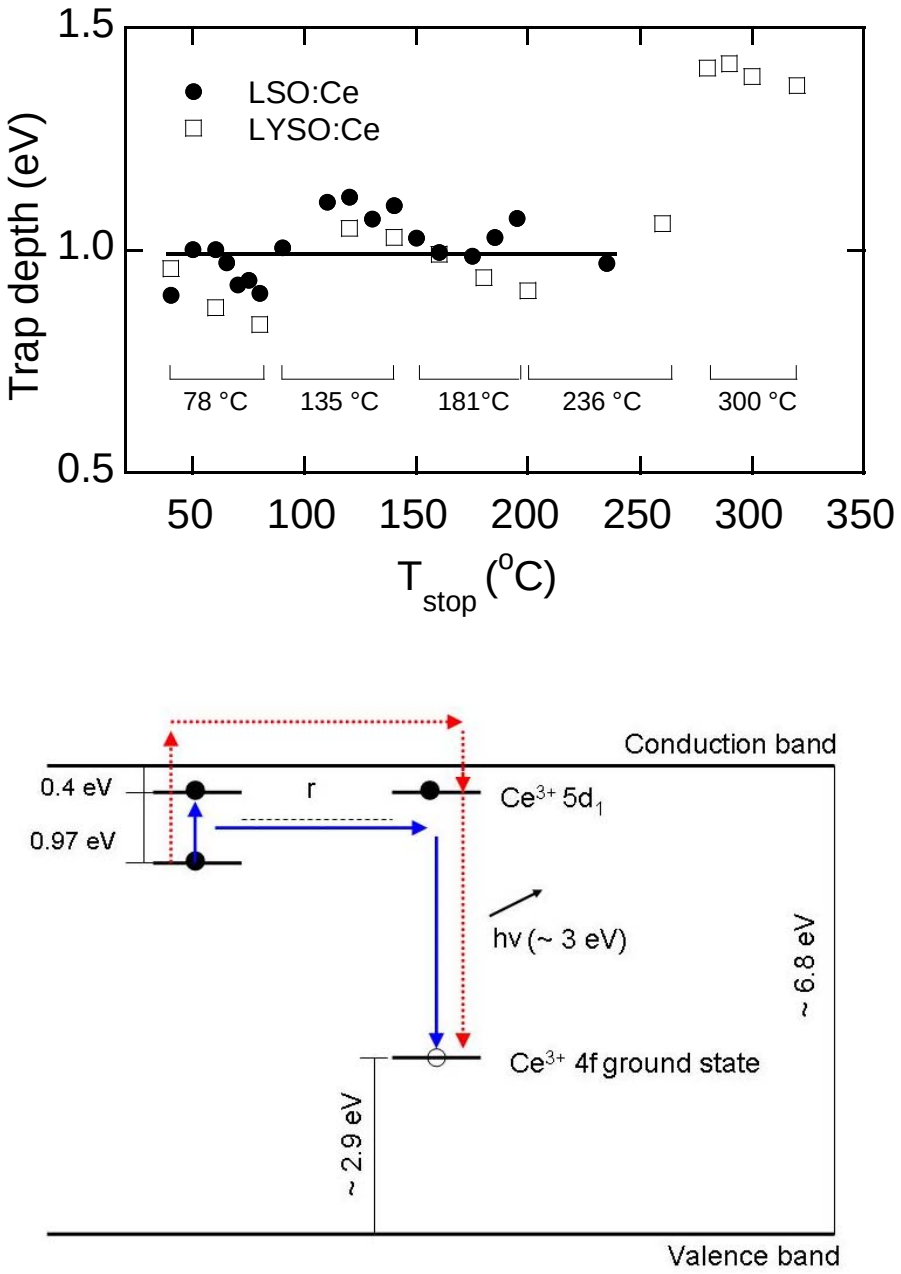

Figure 19 (upper) Trap depths of LSO:Ce and LYSO:Ce evaluated with the initial rise method as a function of T_{stop} temperature. The T_{stop} regions concerning the different glow peaks are marked. (lower) Schematic diagram illustrating the detrapping-recombination processes in LSO and LYSO in the case of Ce doping. In blue (continuous lines), thermally assisted tunnelling recombination; in red (dotted lines), detrapping through the conduction band. See also [P22].

The nature of trapping centers has been further addressed by the focused EPR experiments [P23] in the Y_2SiO_5 single crystals x -ray irradiated at different temperatures: The holes created by irradiation at T < 80 K are firstly self-trapped at Si-unbound oxygen ions forming O^- paramagnetic centers. At T > 80 K, the self-trapped holes become thermally delocalized and then re-trapped at other Si-unbound oxygen ions with perturbing defects (e.g., yttrium vacancies, accidental impurity ions such as P, Mo ions, substituting for Y^{3+} ions, etc.) in their surroundings. As a result, a variety of O^- centers can be created with the thermal stabilities up to room temperatures or even higher. Two of such O^- centers can be ascribed to O^- - V_Y - P_Y and O^- - V_Y - Mo_Y complex defects containing an yttrium vacancy V_Y near an impurity ion. In particular, the ESR spectra of all the O^- centers show the hyperfine structure originating from the interaction of electron spins with the nuclear magnetic moments of neighboring ^{89}Y nuclei.

Besides the O^- hole centers, x-ray irradiation at T < 60 K creates the electron type center. From the analysis of the hyperfine structure of its ESR spectrum, we concluded that an electron is trapped at the Si-unbound O5 vacancy forming thus an F^+ type center. The trapped electrons are assumed to be thermally liberated at 75-90 K without an excitation to the conduction band. The recombination of these electrons with O^--type hole centers is accompanied by thermally stimulated intrinsic visible luminescence.

The identified intrinsic hole and electron centers in YSO structure point to critical importance of the Si-unbound oxygen site in the process of the hole and electron capture in oxyorthosilicates. Our EPR results also confirm the presence of the tunneling mechanism in recombination processes of trapped electrons and holes.

3. General discussion and conclusions

In this thesis a commented review of results from the selected set of papers of the author and his numerous domestic and foreign collaborators is presented. These results are presented in the context of R&D activities all over the world in the field of single crystal scintillators based on the complex oxide compounds, namely the aluminum and multicomponent garnets, aluminum perovskites and pyro and ortho-silicates. In each material family, presented results provide an overlook as for the emission properties of the doped fast luminescence centers, namely Ce^{3+} and Pr^{3+} which enable to obtain the dominant part of scintillation response in the time scale of tens-hundreds of nanoseconds. The problem of trapping charge carriers in the transfer stage of

scintillator mechanism is also clearly demonstrated which introduces in all the materials delayed radiative recombination processes responsible for slower components in scintillation decay and afterglow in time scale of units-tens of microseconds and (longer than) miliseconds, respectively. Considerable effort has been paid to the study of the defects and traps responsible for these unwanted phenomena with quite some success in understanding their nature and relation to the manufacturing technology.

Two modern strategies of the development of novel and/or optimization of existing single crystal scintillators were demonstrated at a number of examples. So called band gap engineering approach consists in the essential change of the electronic band structure of the original material, mostly by alloying it with another component providing a solid solution single crystal material. This strategy appeared extremely productive in the group of garnet scintillators, where balanced admixture of Gd and Ga into the structure of classical $Y_3Al_5O_{12}$ or $Lu_3Al_5O_{12}$ aluminium garnets gave rise to new ultraefficient multicomponent garnet scintillators with light yield approaching 60 000 phot/MeV though at the expense of their temperature stability due to Ce^{3+} excited state ionization early above room temperature. In orthosilicates the Ce-doped LGSO:Ce scintillator can be also considered such a case with comparative advantages in scintillator characteristics around room temperature with respect to both LSO:Ce and GSO:Ce. Also LYSO:Ce is such a case where admixture of YSO component results in better thermal stability of the Ce^{3+} center. Apart from specific changes in the band structure it seems from already several recent examples of cation-mixed compound scintillators [80] that atomistically inhomogeneous arrangement of cations may give rise to local variation of electronic structure of band edges which effectively limits the out-diffusion of charge carrier from ionization track and consequently increases the probability of their radiative recombination, i.e. increases the light yield of such a scintillator. The increase of scintillation efficiency and/or light yield was reported both in the undoped CsI-CsBr and $ZnWO_4$-$MgWO_4$ solid solutions or in the Ce-doped solid solutions of $LaBr_3$-$LaCl_3$, Lu_2SiO_5-Y_2SiO_5, Lu_2SiO_5-Gd_2SiO_5 and $LuAlO_3$-$YAlO_3$. In the most recent case of La-admixed GPS host, such inhomogenities will arise due to atomistic disorder of La and Gd cations at the RE^{3+} site of pyrosilicate structure. Due to the fact that La^{3+} energy levels are expected to provide dominant contribution to the very bottom of conduction band, such an effect is indeed expected.

The second, so called defect engineering strategy has been exploited in a number of cases throughout all the history of scintillators focusing on optimization of particular parameter(s)

important in applications by the suppression or creation of specific defect(s). Doping and codoping by a specific ion often accompanied by post-preparation annealing in a defined (and often proprietary) atmosphere are used for such a purpose. Within last two decades, e.g. (Ce,F) codoping in $Gd_2O_2S:Pr^{3+}$ powder phoshor, $La^{3+}(Y^{3+})$ doping of $PbWO_4$ single crystal and here described Zr^{4+} codoping of YAP:Ce and especially Me^{2+} codoping (Me = Ca, Mg) in Ce-doped orthosilicate and garnet single crystals are successful examples of such material optimization. It is worth noting, however, that these concepts are critically compound-specific and cannot be simply transferred from one material system to another one. In the commented results, probably most interesting and unexpected was revealing the role of stable Ce^{4+} center in scintillation mechanism of Ce-doped garnet single crystal scintilators.

Furthermore, agglomeration of electron traps with Ce^{3+} or Pr^{3+} emission centers was evidenced in practically all material systems under study and becomes almost a general aspect to be always considered [102]: space correlation of trap and recombination center enables tunneling transitions in the radiative electron-hole recombination. It has a significant influence on the timing characteristics of scintillation response and is therefore of great practical importance. Theoretical calculations of electronic band structure or defect creation energy can often provide a guide and indicate possibly promising concepts in such material studies.

It was also the aim of this thesis to demostrate the complexity of R&D of scintillator materials. In fact, it is typical material science field where close collaboration among experts in technology, chemistry, physics and further considering the end-user requirements is truly a must. In several examples above e.g. the correlated use of several experimental techniques from optical and magnetic spectroscopies enabled deep understanding of atomistic aspects of scintillation mechanism, the nature of point defects and related traps and their role in the processes of energy transfer and capture in the host lattice. Such fundamental knowledge is then of great importance in further development and optimization of a particular material system.

Literature - general

[1] G. F. Knoll: *Radiation Detection and Measurement* (Wiley, New York 2000)
[2] D. J. Robbins, *J. Electrochem. Soc.* **1980**, *127*, 2694.
[3] A. Lempicki, A. J. Wojtowicz, E. Berman, *Nucl. Instrum. Methods Phys. Res., Sect. A* **1993**, *333*, 304.
[4] J. Q. Grim, Q. Li, K. B. Ucer, A. Burger, G. A. Bizarri, W. W. Moses, R. T. Williams, *Phys. Status Solidi A* **2012**, *209*, 2421.
[5] P. A. Rodnyi, P. Dorenbos, C. W. E. van Eijk, *Phys. Status Solidi B* **1995**, *187*, 15.
[6] A. N. Vasil'ev, *Nucl. Instrum. Methods Phys. Res., Sect. B* **1996**, *107*, 165.
[7] J. A. Shepherd, S. M. Gruner, M. W. Tate, M. Tecotzky, *Opt. Eng.* **1997**, *36*, 3212.
[8] W. C. Röntgen, *Science* **1896**, *3*, 227.
[9] A. W. Fuchs, *Image* **1960**, *9*, 4.
[10] R. Hofstadter, *Phys. Rev.* **1949**, *75*, 796.
[11] W. van Sciver, R. Hofstadter, *Phys. Rev.* **1951**, *84*, 1062.
[12] M. J. Weber, *J. Lumin.* **2002**, *100*, 35.
[13] R. H. Gilette, *Rev. Sci. Instrum.* **1950**, *21*, 294.
[14] M. J. Weber, R. R. Monchamp, *J. Appl. Phys.* **1973**, *44*, 5495.
[15] A. A. Annenkov, M. V. Korzhik, P. Lecoq, *Nucl. Instrum. Methods Phys. Res., Sect. A* **2002**, *490*, 30.
[16] J. Seco, B. Clasie, M. Partridge, *Phys. Med. Biol.* **2014**, *59*, R303.
[17] C. W. E. van Eijk, *Phys. Med. Biol.* **2002**, *47*, R85.
[18] C. W. E. van Eijk, *Radiat. Prot. Dosim.* **2008**, *129*, 13.
[19] M. Conti, *Phys. Medica* **2009**, *25*, 1.
[20] J. Tous, P. Horodysky, K. Blazek, M. Nikl, J. A. Mares, *J. Instrum.* **2011**, *6,* C01048.
[21] R. C. Runkle, A. Bernstein, P. E. Vanier, *J. Appl. Phys.* **2010**, *108*, 111101.
[22] C. W. E. van Eijk, *IEEE Trans. Nucl. Sci.* **2012**, *59*, 2242.
[23] W. Bachmann, C. Ronda, A. Meijerink, *Chem. Mater.* **2009**, *21,* 2077.
[24] L. H. Brixner, *Mater Chem Phys* **1987**, *16*, 253
[25] M. Ishii, M. Kobayashi, *Prog Cryst Growth Charact Mater* **1992**, *23*, 245
[26] J. Czochralski, J. Phys. Chem. **1918**, *91*, 219
[27] A. Yoshikawa, V. Chani, M. Nikl, *Acta Phys. Pol.* **201**3, *124*, 250.
[28] G. Zhao, X. Zeng, J. Xu, Y. Xu, and Y. Zhou, *J. Cryst. Growth,* **2003**, *253*, 290.
[29] C. D. Brandle, *J. Cryst. Growth* **2004**, *264,* 593.
[30] M. J. Weber, *Solid State Commun.* **1973**, *12*, 741.
[31] R. Autrata, P. Schauer, Jos. Kvapil, J. Kvapil, *J. Phys. E* **1978**, *11*, 707.
[32] M. Moszynski, T. Ludziewski, D. Wolski, W. Klamra, L. O. Norlin, *Nucl. Instrum. Methods Phys. Res. A* **1994**, *345*, 461.
[33] K. V. Ivanovskikh, J. M. Ogiegło, A. Zych, C. R. Ronda, A. Meijerink, *ECS J. Solid State Sci. Technol.* **2013**, *2,* R3148.
[34] W. Chewpraditkul, L. Swiderski, M. Moszynski, T. Szczesniak, A. Syntfeld-Kazuch, C. Wanarak, P. Limsuwan, *IEEE Trans. Nucl. Sci.* **2009**, *56,* 3800.

[35] C.R. Stanek, K.J. McClellan, M.R. Levy, C. Milanese, R.W. Grimes, *Nucl. Instr. Meth. Phys. Research A* **2007**, 579, 27
[36] A. P. Patel, C. R. Stanek, R. W. Grimes, *Phys. Status Solidi B* **2013**, *250*, 1624.
[37] M. Nikl, E. Mihokova, J. Pejchal, A.Vedda, Yu. Zorenko, K. Nejezchleb, *phys. stat. sol. (b)* **2005**, *242***,** R119
[38] C. Dujardin, C. Mancini, D. Amans, G. Ledoux, D. Abler, E. Auffray, P. Lecoq, D. Perrodin, A. Petrosyan, K. L. Ovanesyan, *J. Appl. Phys.* **2010***, 108*, 013510.
[39] K. Kamada, S. Kurosawa, P. Prusa, M. Nikl, V. V. Kochurikhin, T. Endo, K. Tsutumi, H. Sato, Y. Yokota, K. Sugiyama, A. Yoshikawa, *Optical Materials* **2014**, *36*, 1942
[40] P. Dorenbos, *IEEE Trans. Nucl. Sci.* **2010**, *57*, 1162.
[41] A. B. Muñoz-García, L. Seijo, *Phys. Rev. B* **2010***, 82*, 184118.
[42] J. M. Ogiegło, A. Katelnikovas, A. Zych, T. Jüstel, A. Meijerink, C. R. Ronda, *J. Phys. Chem. A* **2013***, 117*, 2479.
[43] J. Ueda, K. Aishima, and S. Tanabe, *Opt. Mater.* **2013***, 35*, 1952.
[44] M. Nikl, K. Kamada, S. Kurosawa, Y. Yokota, A. Yoshikawa, J. Pejchal, V. Babin, *Phys. Stat.sol. (c)* **2013**, *10*, 172
[45] S. R. Rotman, H. L. Tuller, C. Warde, *J. Appl. Phys.* **1992**, *71,* 1209.
[46] S. Liu, X. Feng, Z. Zhou, M. Nikl, Y. Shi, Y. Pan, *Phys. Status Solidi RRL* **2014***, 8,* 105.
[47] Y. Wu, F. Meng, Q. Li, M. Koschan, C. L. Melcher, *Phys. Rev. Applied* **2014**, *2*, 044009.
[48] M. Nikl, V. Babin, J. A. Mares, K. Kamada, S. Kurosawa, A. Yoshikawa, J. Tous, J. Houzvicka, K. Blazek, *The role of cerium variable charge state in the luminescence and scintillation mechanism in complex oxide scintillators,* presented at ICL'2014 conference, 13-18 July 2014, Wroclaw, Poland. Submitted to *J. Lumin*.
[49] M. J. Weber, *J. Appl. Phys.* **1973***,* 44, 3205.
[50] E. G. Gumanskaya, M. V. Korzhik, S. A. Smirnova, V. B. Pavlenko, A. A. Fedorov, *Opt. Spectrosc.* **1992**, *72*, 86.
[51] T. Takeda, T. Miyata, F. Muramatsu, T. Tomiki, *J. Electrochem. Soc.* **1980,** *127*, 438.
[52] E. Autrata, P. Schauer, J. Kvapil, Jos. Kvapil, *Scanning* **1983**, *5*, 91.
[53] D. Klimm, *J. Cryst. Growth* **2010***, 312,* 730.
[54] A. G. Petrosyan, V. F. Popova, V. L. Ugolkov, D. P. Romanov, K. L. Ovanesyan, *J. Cryst. Growth* **2013**, *377*, 178.
[55] J. Trummer, E. Auffray, P. Lecoq, A. Petrosyan, P. Sempere-Roldan, *Nucl. Instrum. Methods Phys. Res., Sect. A* **2005***, 551*, 339.
[56] E. Auffray P. Bruyndonckx, O. Devroede, A. Fedorov, U. Heinrichs, M. Korjik, M. Krieguer, C. Kuntner, C. Lartizien, P. Lecoq, S. Leonard, Ch. Morel, *Nucl. Instrum. Methods Phys. Res., Sect. A* **2004**, *527*, 171.
[57] M. Derdzyana, A. Petrosyan, T. Butaeva, K. Ovanesyan, C. Pedrini, C. Dujardin, N. Garnier, I. Kamenskikh, *Nucl. Instrum. Methods Phys. Res., Sect. A* **2005***, 537*, 200.
[58] W. Drozdowski, A. J. Wojtowicz, T. Lukasiewicz, J. Kisielewski, *Nucl. Instrum. Methods Phys. Res., Sect. A* **2006***, 562*, 254.

[59] A. G. Petrosyan, M. Derdzyan, K. Ovanesyan, P. Lecoq, E. Auffray, J. Trummer, M. Kronberger, C. Pedrini, C. Dujardin, P. Anfre, *Nucl. Instrum. Methods Phys. Res., Sect. A* **2007**, *571*, 325.
[60] K. Kamada, T. Endo, K. Tsutsumi, A. Yoshikawa, (2012) *Phys. Status Solidi C* **2012**, *9*, 2263.
[61] A. Yamaji, V. Kochurikhin, Y. Fujimoto, Y. Futami, T. Yanagida, Y. Yokota, S. Kurosawa, A. Yoshikawa, *Phys. Status Solidi C* **2012**, *9*, 2267.
[62] P. Lecoq, A. Annenkov, A. Gektin, M. Korzhik, C. Pedrini, *Inorganic Scintillators for Detector Systems: Physical Principles and Crystal Engineering*, Springer, Heidelberg, Germany 2006
[63] M. Zhuravleva, A. Novoselov, E. Mihokova, J. A. Mares, A. Vedda, M. Nikl, A. Yoshikawa, *IEEE Trans. Nucl. Sci.* **2008**, *55*, 1476.
[64] C. W. E. van Eijk, P. Dorenbos, R. Visser, *IEEE Trans. Nucl. Sci.* **1994**, 41, 738.
[65] O. F. Schirmer, K. W. Blazey, W. Berlinger, *Phys. Rev. B* **1975**, *11*, 4201.
[66] A.Vedda, M.Martini, F.Meinardi, J.A. Mares, E.Mihokova, J.Chval, M.Dusek, M.Nikl, Phys. Rev. B **2000**, *61*, 8081.
[67] C. R. Stanek, K. J. McClellan, M. R. Levy, R. W. Grimes, J. Appl. Physics **2006**, *99*, 113518
[68] K. Takagi, T. Fukazawa, *Appl. Phys. Lett.* **1983**, *42*, 43.
[69] C. L. Melcher, J. S. Schweitzer, *Nucl. Instrum. Methods Phys. Res., Sect. A* **1992**, *314*, 212.
[70] H. Suzuki, T. A. Tombrello, C. L. Melcher, J. S. Schweitzer, *Nucl. Instrum. Methods Phys. Res., Sect. A* **1992**, *320*, 263.
[71] M. Kokubun, K. Abe, Y. Ezoe, Y. Fukazawa, S. Hong, H. Inoue, T. Itoh, T. Kamae, D. Kasama, M. Kawaharada, et al., *IEEE Trans. Nucl. Sci.* **2004**, *51*, 1991.
[72] D. W. Cooke, K. J. McClellan, B. L. Bennett, J. M. Roper, M. T. Whittaker, R. E. Muenchausen, R. C. Sze, *J. Appl. Phys.* **2000**, *88*, 7360.
[73] L. Qin, H. Li, S. Lu, D. Ding, G. Ren, *J. Cryst. Growth* **2005**, *281*, 518.
[74] E. van der Kolk, S. A. Basun, G. F. Imbush, W. M. Yen, *Appl. Phys. Lett.* **2003**, *83*, 1740.
[75] M. Nikl, H. Ogino, A. Yoshikawa, E. Mihokova, J. Pejchal, A. Beitlerova, A. Novoselov, T. Fukuda, *Chem. Phys. Letters* **2005**, *410*, 218
[76] G. B. Loutts, A. I. Zagumenni, S. V. Lavrishichev, Y. D. Zavartsev, P. A. Studenikin, *J. Cryst. Growth* **1997**, *174*, 331.
[77] T. Usui, S. Shimizu, N. Shimura, K. Kurashige, Y. Kurata, H. Ishibashi, H. Yamamoto, *IEEE Nucl. Sci. Symp. Conf. Rec.* **2006**, *2*, 1166.
[78] O. Sidletskiy et al., *J. Cryst. Growth* **2010**, *312*, 601.
[79] O. Sidletskiy et al., *Cryst. Growth Des.* **2012**, *12*, 4411.
[80] A. Gektin, A. Belsky, A. Vasil'ev, *IEEE Trans. Nucl. Sci.* **2014**, *61*, 262.
[81] M. A. Spurrier, P. Szupryczynski, K. Yang, A. A. Carey, C. L. Melcher, *IEEE Trans Nucl. Sci.* **2008**, *55*, 1178.

[82] K. Yang, C. L. Melcher, P. D. Rack, L. A. Eriksson, *IEEE Trans Nucl. Sci.* **2009**, *56*, 2960.
[83] H. E. Rothfuss, C. L. Melcher, L. A. Eriksson, M. A. Spurrier Koschan, *IEEE Trans. Nucl. Sci.* **2009**, *56*, 958.
[84] S. Blahuta, A. Bessiere, B. Viana, P. Dorenbos, V. Ouspenski, V. *IEEE. Trans. Nucl. Sci.* **2013**, *60*, 3134.
[85] R. Visser, C. L. Melcher, J. S. Schweizer, H. Suzuki, T. A. Tombrello, *IEEE Trans. Nucl. Sci.* **1994**, *41*, 689.
[86] F. Moretti, A. Vedda, N. Chiodini, M. Fasoli, A. Lauria, V. Jary, R. Kucerkova, Mihokova, A. Nale, M. Nikl, *J. Lumin.* **2012**, *132*, 461.
[87] B. Chai, U. S. Patent No. 7151261, **2006**
[88] D. Pauwels, N. Le Masson, B. Viana, A. Kahn-Harari, E. V. D. van Loef, P. Dorenbos, C. W. E. van Eijk, *IEEE Trans. Nucl. Sci.* **2000**, *47*, 1787.
[89] L. Pidol, O. Guillot-Noël, A. Kahn-Harari, B. Viana, D. Pelenc, D. J. Gourier, *Phys. Chem. Solids* **2006**, *67*, 643.
[90] L. Pidol, A. Kahn-Harari, B. Viana, E. Virey, B. Ferrand, P. Dorenbos, J. T. M. De Haas, C. W. E. van Eijk, *IEEE Trans. Nucl. Sci.* **2004**, *51*, 1084.
[91] H. Feng, D. Ding, H. Li, S. Lu, S. Pan, X. Chen, G. Ren, *J. Appl. Phys.* **2008**, *103*, 083109.
[92] L. Pidol, A. Kahn-Harari, B. Viana, B. Ferrand, P. Dorenbos, J. T. M. De Haas, C. W. E. van Eijk, E. Virey, *J. Phys.: Condens. Matter* **2003**, *15*, 2091.
[93] S. Kawamura, J. H. Kaneko, M. Higuchi, F. Fujita, A. Homma, J. Haruna, S. Saeki, K. Kurashige, H. Ishibashi, M. Furusaka, *Nucl. Instrum. Methods Phys. Res., Sect. A* **2007,** *583***,** 356.
[94] N. A. Toropov, F. Ya. Glakhov, S. F. Konovalova, *Russ. Chem. Bull.* **1961**, *10*, 497.
[95] S. Kawamura, J. H. Kaneko, M. Higuchi, T. Yamaguchi, J. Haruna, Y. Yagi, K. Susa, F. Fujita, A. Homma, S. Nishiyama et al., *IEEE Nucl. Sci. Symp. Conf. Rec.* **2006**, *2*, 1160.
[96] A. Suzuki, S. Kurosawa, T. Shishido, J. Pejchal, Y. Yokota, Y. Futami, A. Yoshikawa, *Appl. Phys. Express* **2012**, *5*, 102601.
[97] S. Kurosawa, T. Shishido, A. Suzuki, J. Pejchal, Y. Yokota, A. Yoshikawa, *Nucl. Instrum. Methods Phys. Res., Sect. A* **2014**, *744*, 30.
[98] Y. A. Gerasymov, V. Baumer, S. Neicheva, N. Starzhinskiy, V. Tarasov, O. Zelenskaya, O. Sidleskiy, *Funct. Mater.* **2013**, 20, 15.
[99] W. Chewpraditkul, C. Wanarak, T. Szczesniak, M. Moszynski, V. Jary, A. Beitlerova, M. Nikl, *Opt. Mater.* **2013**, *35*, 1679.
[100] P. Dorenbos, C. W. W. van Eijk, A. J. J. Bos, C. L. Melcher, *J. Phys.Cond. Matter* **1994**, *6*, 4167
[101] R. Visser, C. L. Melcher, J. S. Schweizer, H. Suzuki, T. A. Tombrello, *IEEE Trans. Nucl. Sci.* **1994**, *41*, 689
[102] F. Clabau, X. Rocquefelte, T. Le Mercier, P. Deniard, S. Jobic, M.-H. Whangbo. Chem. Mater. **2006,** *18,* 3212

Literature – commented author's paper selection

P1. M.Nikl, E.Mihokova, J.A.Mares, A.Vedda, M.Martini, K.Nejezchleb, K.Blazek: *Traps and timing characteristics of LuAG:Ce^{3+} scintillator.* phys.stat.sol. (b) **181**, R10-R12 (2000). https://doi.org/10.1002/1521-396X(200009)181:1<R10::AID-PSSA999910>3.0.CO;2-9

P2. M. Nikl, H. Ogino, A.Krasnikov, A. Beitlerova, A.Yoshikawa and T. Fukuda. *Photo- and radioluminescence of Pr-doped $Lu_3Al_5O_{12}$ single crystal.* Phys. Stat.sol. (a) **202**, R4-R6 (2005). https://doi.org/10.1002/pssa.200409079

P3. M. Nikl, K. Kamada, V. Babin, J. Pejchal, K. Pilarova, E. Mihokova, A. Beitlerova, K. Bartosiewicz, S. Kurosawa, A. Yoshikawa, *Defect-engineering in Ce-doped aluminum garnet single crystal scintillators.* Cryst. Growth Des. **14**, 4827-4833 (2014). https://pubs.acs.org/doi/10.1021/cg501005s

P4. M. Nikl, J. A. Mares, N. Solovieva, J. Hybler, A. Voloshinovskii, K. Nejezchleb, K. Blazek, *Energy transfer to the Ce^{3+} centers in $Lu_3Al_5O_{12}$:Ce scintillator. Phys. Status Solidi A* **201**, R41-R44 (2004). https://doi.org/10.1002/pssa.200409041

P5. M. Nikl, A. Vedda, M. Fasoli, I. Fontana, V. V. Laguta, E. Mihokova, J. Pejchal, J. Rosa, K. Nejezchleb, *Shallow traps and radiative recombination processes in $Lu_3Al_5O_{12}$:Ce single crystal scintillator*. Phys. Rev. B **76**, 195121 (2007). https://journals.aps.org/prb/abstract/10.1103/PhysRevB.76.195121

P6. M. Nikl, E. Mihokova, J. Pejchal, A. Vedda, M. Fasoli, I. Fontana, V. V. Laguta, V. Babin, K. Nejezchleb, A. Yoshikawa, H. Ogino, and G. Ren, *Scintillator Materials—Achievements, Opportunities, and Puzzles.* IEEE Trans. Nucl. Sci. **55**, 1035-1041 (2008). (invited talk at SCINT2007 conference). https://ieeexplore.ieee.org/document/4545180

P7. M.Nikl, A. Yoshikawa, K. Kamada, K. Nejezchleb, C.R. Stanek, J.A. Mares, K. Blazek, *Development of LuAG-based Scintillator Crystals - A Review*. Progr. Cryst. Growth Charact. Materials **59,** 47-72 (2013). http://dx.doi.org/10.1016/j.pcrysgrow.2013.02.001

P8. K. Kamada , T. Yanagida , T. Endo , K. Tsutumi , Y. Fujimoto , A. Fukabori, A. Yoshikawa, J. Pejchal, M. Nikl, *Composition engineering in Ce doped $(Lu,Gd)_3(Ga,Al)_5O_{12}$ single crystal scintillators.* Crystal Growth & Design **11**, 4484-4490 (2011). http://dx.doi.org/10.1021/cg200694a

P9. K. Kamada, T. Yanagida, J. Pejchal, M. Nikl, T. Endo, K. Tsutumi, Y. Fujimoto, A. Fukabori, A. Yoshikawa, *Scintillator-oriented combinatorial search in the Ce doped $(Y,Gd)_3(Ga,Al)_5O_{12}$ multicomponent garnet compounds.* J. Phys. D: Appl. Phys. **44** 505104 (2011). http://dx.doi.org/10.1088/0022-3727/44/50/505104

P10. M. Fasoli, A. Vedda, M. Nikl, C. Jiang, B. P. Uberuaga, D. A. Andersson, K. J. McClellan, C. R. Stanek, *Band gap engineering for shallow trap removal in $RE_3Al_5O_{12}$ garnets.* Phys. Rev. B **84**, 081102(R) (2011). http://dx.doi.org/10.1103/PhysRevB.84.081102

P11. K. Kamada, M. Nikl, S. Kurosawa, A. Beitlerova, A. Nagura; Y. Shoji, J. Pejchal, Y. Ohashi, Y. Yokota, A. Yoshikawa, *Alkali Earth Co-doping Effects on Luminescence and Scintillation Properties of Ce doped $Gd_3Al_2Ga_3O_{12}$ scintillator.* Opt. Mater.(2015), DOI 10.1016/j.optmat.2014.10.008 . http://dx.doi.org/10.1016/j.optmat.2014.10.008

P12. K. Blazek, A. Krasnikov, K. Nejezchleb, M. Nikl, T. Savikhina and S.Zazubovich, *Luminescence and defect creation in Ce^{3+}-doped $YAlO_3$ and $Lu_{0.3}Y_{0.7}AlO_3$ crystals.* Phys. Stat.sol. (b) **242**, 1315-1323 (2005). http://dx.doi.org/10.1002/pssb.200440004

P13. E. Mihóková, M. Nikl, M. Bacci, M. Dušek, V. Petříček, *Assignment of 4f-5d absorption bands in Ce-doped $RAlO_3$ (R=La, Gd, Y, Lu) hosts*. Phys. Rev. B **79**, 195130 (2009). http://dx.doi.org/10.1103/PhysRevB.79.195130

P14. M. Nikl, J. A. Mares, A. Vedda, M. Fasoli, V. Laguta, E. Mihokova, J. Pejchal, M. Zhuravleva, A. Yoshikawa, K. Nejezchleb, , *Can Pr-doped YAP scintillator perform better?* IEEE Trans. Nucl. Sci. **57** 1168-1174 (2010).(invited talk at SCINT2009 conference) http://dx.doi.org/10.1109/TNS.2010.2043116

P15. A. Vedda, M. Fasoli, M. Nikl, V. V. Laguta, E. Mihokova, J. Pejchal, A. Yoshikawa, M. Zhuravleva, *Trap-Centre Recombination Processes by Rare Earth Activators in $YAlO_3$ Single Crystal Host.* Phys. Rev. B **80**, 045113 (2009). http://dx.doi.org/10.1103/PhysRevB.80.045113

P16. V. V. Laguta, M. Nikl, A. Vedda, E. Mihokova, J. Rosa, K. Blazek, *The hole and electron traps in the $YAlO_3$ single crystal scintillator*. Phys. Rev. B **80,** 045114 (10 pp) (2009). http://dx.doi.org/ 10.1103/PhysRevB.80.045114

P17. M.Nikl, J.A.Mares, J.Chval, E.Mihokova, N.Solovieva, M.Martini, A.Vedda, K.Blazek, P.Maly, K.Nejezchleb, P.Fabeni, G.P.Pazzi, V.Babin, K.Kalder, A.Krasnikov, S.Zazubovich, C.D'Ambrosio: *An effect of Zr^{4+} co-doping of YAP:Ce scintillator.* Nucl.Instr.Meth. Phys.Research A **486**, 250-253 (2002). https://www.sciencedirect.com/science/article/pii/S0168900202007118

P18. V. Jarý, E. Mihóková, J. A. Mareš, A. Beitlerová, D. Kurtsev, O. Sidletskiy, M. Nikl, *Comparison of the scintillation and luminescence properties of the $(Lu_{1-x}Gd_x)_2SiO_5$:Ce single crystal scintillators.* J. Phys. D: Appl. Phys. **47** 365304 (2014). http://dx.doi.org/10.1088/0022-3727/47/36/365304

P19. H. Feng, V. Jary, E. Mihokova, D. Ding, M. Nikl , G. Ren, H. Li, S. Pan, A. Beitlerova, R. Kucerkova, *Temperature dependence of luminescence characteristics of LYSO:Ce scintillator grown by the Czochralski method*. J. Appl. Physics **108,** 033519 (2010). http://dx.doi.org/10.1063/1.3457856

P20. V. Jary, M. Nikl, S. Kurosawa, Y. Shoji, E. Mihokova, A. Beitlerova, G. P. Pazzi, A. Yoshikawa, *Influence of yttrium Content on the Ce1 and Ce2 Luminescence Characteristics in$(Lu_{1-x}Y_x)_2SiO_5$:Ce Single Crystals*. IEEE Trans. Nucl. Science **59**, 2079 - 2084 (2012). https://ieeexplore.ieee.org/document/6187676

P21. V. Jary, M. Nikl, S. Kurosawa, Y. Shoji, E. Mihokova, A. Beitlerova, G. P. Pazzi, A. Yoshikawa, *Luminescence Characteristics of the Ce^{3+}-Doped Pyrosilicates: The Case of La-Admixed $Gd_2Si_2O_7$ Single Crystals.* J. Phys. Chemistry C **118** , 26521–26529 (2014). http://dx.doi.org/10.1021/jp5080384

P22. A. Vedda, M. Nikl, M. Fasoli, E. Mihokova , J. Pejchal, M. Dusek, G. Ren, C.R. Stanek, K. J. McClellan, D.D. Byler, *Thermally Stimulated Tunnelling in Rare-Earth Doped Lu-Y Oxyorthosilicates*. Phys. Rev. **B 78,** 195123 (2008). http://dx.doi.org/10.1103/PhysRevB.78.195123

P23. V.V. Laguta, M. Buryi, J. Rosa, D. Savchenko, J. Hybler, M. Nikl, S. Zazubovich, T. Kärner, C.R. Stanek, K.J. McClellan, *Electron and hole traps in yttrium orthosilicate single crystals: the critical role of Si-unbound oxygen.* Phys. Rev. B **90**, 064104 (2014). http://dx.doi.org/10.1103/PhysRevB.90.064104

Literature – author's invited papers and book chapter related to the topic of theses

V1. M. Nikl, *Scintillation detectors for X-rays.* Meas. Sci. Technol. **17**, R37-R54 (2006)

V2. M. Nikl, *WIDE BAND GAP SCINTILLATION MATERIALS. Progress in the technology and material understanding.* phys.stat.sol. (a) **178**, 595-620 (2000)

V3. M. Nikl, A. Vedda, V. V. Laguta, in *Springer Handbook of Crystal Growth* (Eds: G. Dhanaraj, K. Byrappa, V. Prasad, M. Dudley) Springer, Heidelberg, GE **2010**, pp. 1663-1700.

Reprints of commented author's paper selection

Can be obtained at web links provided in the list.